Precursory seismic quiescence before the M_w = 8.3 Tokachi-oki, Japan, earthquake on 26 September 2003 revealed by a re-examined earthquake catalog

Kei Katsumata[1]

Received 1 September 2010; revised 26 April 2011; accepted 20 July 2011; published 15 October 2011.

[1] The 2003 Tokachi-oki earthquake (M_w = 8.3) occurred on 26 September 2003 off the pacific coast of Hokkaido, Japan. In the present study, an earthquake catalog is used that lists 2,000 earthquakes with $M \geq 3.3$. All of the earthquake waveforms were recorded by the Institute of Seismology and Volcanology, Hokkaido University. In the present study, these waveforms are manually re-examined, and hypocenters and magnitudes are re-calculated. A detailed analysis of the re-determined earthquake catalog between 1994 and 2003 using a gridding technique (ZMAP) shows that the 2003 Tokachi-oki earthquake is preceded by two neighboring seismic quiescence anomalies that start around the beginning of 1999, and last about 5 years, until the main shock occurs. These quiescence anomalies are located around the asperity ruptured by the main shock, and the Z-values are +3.9 and +4.0 for a time window of T_w = 4 years, using a sample size of N = 100 earthquakes. The detected seismic quiescences can be interpreted as being caused by a decrease of 50% in the stressing rate based on Dieterich's theory. It is proposed that a quasi-static pre-slip occurs at the northeastern edge of the asperity ruptured by the main shock, and lasts for five years until the main shock occurs. By calculating the change in the Coulomb failure stress (ΔCFS), it is found that negative ΔCFS areas are consistent with the two quiescence anomalies, and a positive ΔCFS area corresponds to the hypocenter of the main shock, indicating that the quasi-static pre-slip model is a plausible one.

Citation: Katsumata, K. (2011), Precursory seismic quiescence before the M_w = 8.3 Tokachi-oki, Japan, earthquake on 26 September 2003 revealed by a re-examined earthquake catalog, *J. Geophys. Res.*, *116*, B10307, doi:10.1029/2010JB007964.

1. Introduction

[2] Several significant cases support the hypothesis that seismic quiescence precedes the occurrence of large earthquakes [e.g., *Mogi*, 1969; *Ohtake et al.*, 1977; *Wyss*, 1985]. *Wyss and Habermann* [1988] summarized seventeen cases of precursory seismic quiescence preceding main shocks with magnitudes ranging from M = 4.7 to 8.0, and found that (1) the rate of decrease ranged from 45% to 90%, (2) the duration of the precursors ranged from 15 to 75 months, (3) if a false alarm was defined as a period of quiescence with a significance level larger than a precursory quiescence in the same tectonic area, the false alarm rate might be in the order of 50%, and (4) failure to predict might be expected in 50% of the main shocks, even in carefully monitored areas. Among the seventeen cases, there were three which could be considered successful predictions in the sense that a quiescence anomaly was recognized and interpreted as a precursor before the occurrence of the main shock [*Ohtake et al.*, 1977; *Kisslinger*, 1988; *Wyss and Burford*, 1985; *Wyss and Burford*, 1987]. Recently, more reliable examples of seismic quiescence have been reported: the Spitak earthquake (M = 7.0) in 1988 [*Wyss and Martirosyan*, 1998], the Landerse earthquake (M = 7.5) in 1992 [*Wiemer and Wyss*, 1994], the Hokkaido-Toho-oki earthquake (M_w = 8.3) in 1994 [*Katsumata and Kasahara*, 1999], the Hyogo-ken Nanbu earthquake (M = 7.3) in 1995 [*Enescu and Ito*, 2001]. However, it is not yet clear how common this phenomenon is, what its characteristics are, and how it can best be measured quantitatively. The purpose of the present study is to document in detail a case history of precursory quiescence before the Tokachi-oki earthquake (M_w = 8.3) in 2003 based on a carefully re-examined earthquake catalog.

[3] A great earthquake occurred at 4:50 A.M. on 26 September 2003 (Japan Standard Time) off the pacific coast of Hokkaido, Japan (Figure 1). The earthquake was named the 2003 Tokachi-oki earthquake by the Japan Meteorological Agency (JMA). The location of the hypocenter, determined by the Institute of Seismology and Volcanology, Hokkaido University (ISV), was 41.86°N, 144.09°E and 28 km in depth. According to the Global CMT solution, the focal mechanism was a low-angle thrust type and the seismic moment was $M_0 = 3.0 \times 10^{21}$ Nm (M_w = 8.3), whereas the JMA magnitude was 8.0. This remarkable event was a typical

[1]Institute of Seismology and Volcanology, Hokkaido University, Sapporo, Japan.

0148-0227/11/2010JB007964

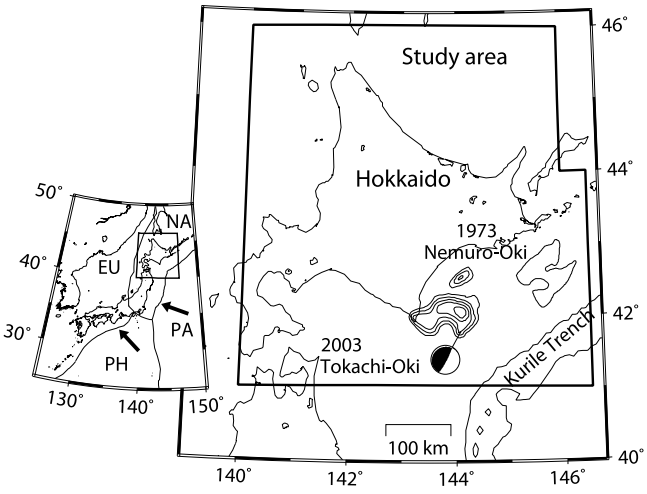

Figure 1. Hokkaido subduction zone. The bold solid line indicates the study area. The focal mechanism is shown for the 2003 Tokachi-oki earthquake (M_w = 8.3). Asperities are indicated by contours every 1 m of displacement on the faults for the Tokachi-oki and the Nemuro-oki earthquakes [*Yamanaka and Kikuchi*, 2003]. Six and seven kilometers contours at the Kurile Trench show the ocean bottom topography. The inset shows plate boundaries: the Eurasian (EU), Pacific (PA), North American (NA) and Philippine Sea (PH) plates. Arrows indicate the direction of plate motion relative to the Eurasian plate.

subduction zone earthquake on the interface between the Pacific and the North American plates. The 2003 Tokachi-oki earthquake ruptured the same asperities as those ruptured by the 1952 Tokachi-oki earthquake [e.g., *Yamanaka and Kikuchi*, 2003; *Yagi*, 2004; *Hamada and Suzuki*, 2004]. A large tsunami [*Hirata et al.*, 2004; *Tanioka et al.*, 2004] and many aftershocks [*Shinohara et al.*, 2004] followed the main shock. An outstanding afterslip was also observed by a dense GPS network (GPS Earth Observation Network; GEONET). The afterslip was distributed mainly in the surrounding areas of co-seismic slip [*Ozawa et al.*, 2004; *Miyazaki et al.*, 2004; *Baba et al.*, 2006]. A pre-slip immediately before the main shock was suggested based on precise leveling observations before the 1944 Tonankai earthquake [*Mogi*, 1985; *Linde and Sacks*, 2002]. However, no precursory anomaly was detected by tilt-meter, 1-Hz GPS, or groundwater measurements before the 2003 Tokachi-oki earthquake [*Hirose*, 2004; *Irwin et al.*, 2004; *Sato et al.*, 2004], and no foreshock activity was observed. On the other hand, it is noteworthy that anomalous VHF-band radio waves were observed prior to the main shock [*Moriya et al.*, 2010].

[4] Whereas the detection of pre-slip is a crucial key to successful earthquake prediction, there was no detectable precursory slip anomaly immediately before the 2003 Tokachi-oki earthquake. Therefore, the seismic quiescence hypothesis should be tested as an intermediate-term precursor candidate for this great earthquake. However, there are important shortcomings for investigating precise and reliable changes in long-term seismicity. The homogeneity of an earthquake catalog is critical for the analysis of seismic quiescence and, in general, most catalogs are not homogeneous temporally and spatially [*Habermann*, 1987, 1991]. For this reason, a homogeneous earthquake catalog should be constructed prior to such an analysis. Apparent changes in seismicity rates are easily produced by artificial effects, including deployment of new seismograph stations, closing of old seismograph stations, changes to the seismograph, waveform-recording system, and magnitude estimation algorithm [*Habermann and Creamer*, 1994; *Zuniga and Wiemer*, 1999]. For example, improvement of the coverage by adding additional seismic stations leads to the detection and location of smaller earthquakes, and the seismicity rate would therefore appear to increase as a function of time. It might be assumed that a catalog of large earthquakes is temporally homogeneous because there is no change in the detection rate for these earthquakes. However, systematic changes such as those described below can affect all magnitude bands so that an earthquake catalog should not be used without a carful check for homogeneity in space and time.

[5] There are two types of systematic changes in magnitude that should be carefully checked. The first is a magnitude shift, in which all magnitudes are offset by the same amount. The second is a magnitude stretch, in which different magnitudes are offset by different amounts. The Gutenberg-Richter relation [*Ishimoto and Iida*, 1939; *Gutenberg and Richter*, 1944] is one of the well-fitted empirical relations in seismology: it represents the frequency of occurrence of earthquakes as a function of magnitude: $\log_{10}N = a - bM$, where N is the cumulative number of earthquakes with magnitude larger than M and a and b are constants. There have in fact been two case studies in which man-made changes in the b-value occurred in the Hokkaido region. A temporal change in b-value means that a magnitude shift and/or stretch has occurred. *Katsumata and Kasahara* [1999] found an apparent change in the b-value in an earthquake catalog produced by ISV. A new data acquisition system called the WIN-SYSTEM [*Urabe and Tsukada*, 1992] was installed at ISV in May 1993. Subsequently, the b-value shifted drastically from 1.4 to 0.8 for the seismicity in the Kurile Islands between 144°E and 149°E. *Katsumata and Kasahara* [2004] also found an apparent change in the b-value caused by an increase in the number of short-period seismographic stations from approximately 60 to 120 in November 1996. This was due to the unification of the two seismographic networks of ISV and JMA. At that time, the b-value decreased from 0.78 to 0.72, which was statistically significant based on Utsu's test [*Utsu*, 1999].

[6] In the present study, all waveform data are first carefully re-examined and hypocenters and magnitudes are re-determined in order to obtain a reliable earthquake catalog that is homogeneous spatially and temporally. Seismic quiescence prior to the 2003 Tokachi-oki earthquake is then defined quantitatively using an algorithm in the program ZMAP [*Wiemer*, 2001]. A numerical simulation is then performed to estimate the statistical significance of the quiescence obtained. Finally, whether or not the seismic quiescence is a precursor to the 2003 Tokachi-oki earthquake is discussed.

2. Data

[7] As described in the previous section, the most important requirement for a seismic quiescence analysis is the use of a homogeneous earthquake catalog. Recently, many new seismographic stations have been installed in the Hokkaido region. At present, the ISV network consists of about 240 short-period

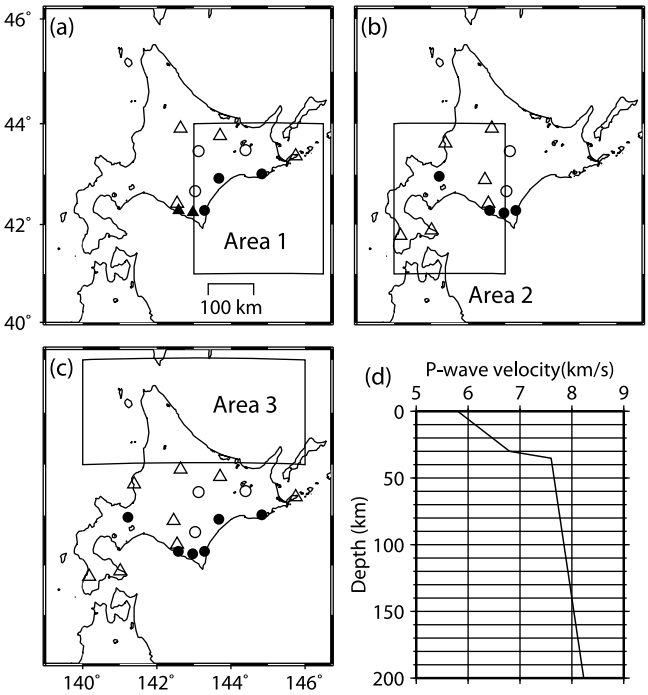

Figure 2. (a–c) Seismographic stations used in the relocation of hypocenters. Arrival times of *P* waves only at the stations indicated by open and closed triangles are used. Arrival times of both *P* and *S* waves are used at the stations indicated by open and closed circles. Magnitudes are calculated from the maximum amplitude at the stations indicated by closed circles and closed triangles. The study area is divided into three: Area 1 (41°–44°N, 143°–146.5°E), Area 2 (41°–44°N, 140°–143°E) and Area 3 (44°–46°N, 140°–146°E). (d) *P* wave velocity structure used for hypocenter location in the study area, which is the same as that used for the hypocenter calculation in the ISV data processing system [*Suzuki et al.*, 1988; *Katsumata et al.*, 2003]. Poisson's ratio is assumed to be 0.25 in each layer.

seismograph stations, including Hi-net (the high-sensitivity seismographic network) and JMA stations. All the waveform data are converted to digital form at 100 Hz, sent to the ISV via a communication satellite, exclusive telephone lines or an Internet connection, and stored on both hard disks and 8 mm video tapes.

[8] In the present study, earthquakes are selected from the ISV catalog that satisfy the following conditions: (1) they occurred between 1 January 1994 and 25 September 2003, (2) they are located in the study area shown in Figure 1, (3) they have magnitudes $M \geq 3.0$, (4) five or more *P* wave arrival times are available, and (5) two or more *S* wave arrival times are available. Approximately 90,000 events satisfy conditions (1) and (2). Among these, 5,719 events satisfy conditions (3), (4), and (5), and the waveforms associated with these events are re-examined.

[9] The study area is divided into three, labeled Area 1, Area 2 and Area 3 in Figure 2. The earthquakes in these areas are relocated using stations which were deployed before 1994, and there have been no change in the observation conditions up to the present. Data from any station installed after 1994 are not used in this process, in order to preserve the homogeneity of the earthquake catalog. For Area 1, the arrival times of *P* waves are determined from the vertical component at all 12 stations in Figure 2a. The arrival times of *S* waves are determined from the horizontal component at the 6 stations indicated by open and closed circles in Figure 2a. The hypocenters are then determined from the arrival time data using the program HYPOMH, which is based on a simple algorithm to find the maximum likelihood solution using a Bayesian approach [*Hirata and Matsu'ura*, 1987]. The one-dimensional *P* wave velocity model shown in Figure 2d is used; this is the same as that used for hypocenter calculations in the ISV data processing system [*Suzuki et al.*, 1988; *Katsumata et al.*, 2003]. The *S* wave velocity is determined by assuming that $V_p/V_s = \sqrt{3}$, where V_p and V_s are the *P* and *S* wave velocities, respectively. This is equivalent to assuming that the Poisson's ratio is 0.25. A value of 0.25 applies mainly to crustal structures, whereas values in the mantle are typically higher (approximately 0.28). In general, this ratio varies with changes in material composition. The maximum amplitudes are measured on the vertical component at the 5 stations indicated by closed circles and closed triangles in Figure 2a. The magnitude M_i is calculated at each station by using the equation

$$0.85M_i - 2.50 = \log A_v + 1.73 \log r,$$

where A_v is the maximum amplitude in cm/s and r is an epicentral distance in km [*Watanabe*, 1971]. The magnitude of an earthquake is obtained by averaging the M_i values for the 5 stations where the maximum amplitudes are measured. The same procedure is carried out for Areas 2 and 3 using a different group of seismograph stations.

[10] The Pacific plate subducts beneath Hokkaido in a direction from southeast to northwest along the Kurile Trench (see Figure 1). Taking the depth location error into account, a new boundary is defined that is 5 km shallower than the upper surface of the deep seismic zone presented by *Katsumata et al.* [2003, Figure 10a]. From the re-examined earthquake catalog, earthquakes deeper than this new boundary are selected to analyze the seismicity within the Pacific plate. Earthquakes occurring in the inland crust are removed.

[11] Two thousand earthquakes are then selected which satisfy the following conditions: (1) the epicenters are located west of 146°E, (2) the depth is shallower than 200 km, and (3) the magnitude is equal to or larger than 3.3. These 2,000 earthquakes then form the basis of this analysis (Figures 3a and 3b). In this study, clustered events such as aftershocks and earthquake swarms are not removed because the declustering of an earthquake catalog is a non-unique procedure with well-known shortcomings [*Zhuang et al.*, 2002]. On the other hand, many previous seismicity studies using *Z*-value statistics [e.g., *Wyss and Martirosyan*, 1998; *Enescu and Ito*, 2001] have argued for the necessity of declustering. However, even if such declustering is carried out, only about 3% of events are removed, which would not change the conclusions reached in the present study. The number of earthquakes versus magnitude is then examined for the catalog to estimate the magnitude of completeness, M_C. In this study, M_C is defined as the magnitude at which at least 90% of the frequency-magnitude distribution can be modeled using a power law [*Wiemer and Wyss*, 2000]. The results indicate that almost all earthquakes with $M \geq 3.3$ can be located without fail, that is, $M_C = 3.3$, and there is no temporal change in M_C

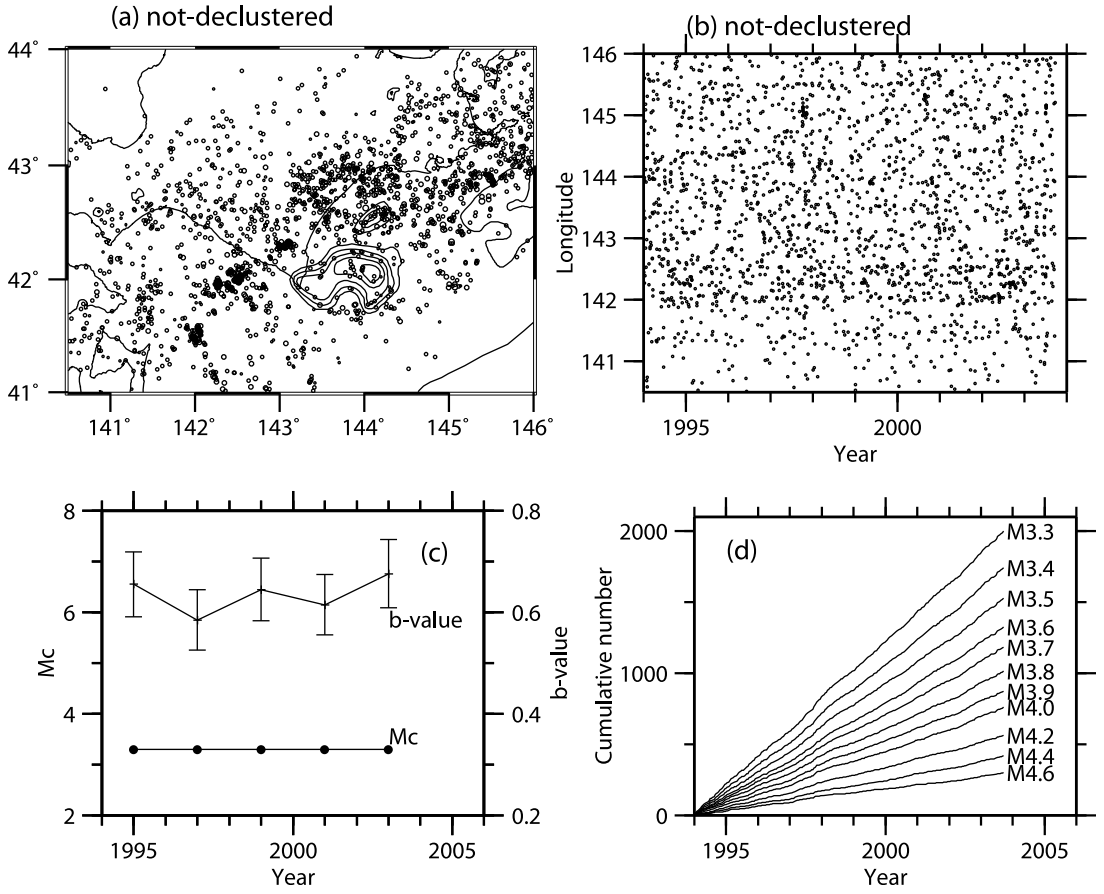

Figure 3. (a) Epicenters of earthquakes used in this study located within the Pacific plate (1 January 1994–25 September 2003, M ≥ 3.3, 0 ≤ Depth (km) ≤ 200). This earthquake catalog includes clustered events such as aftershocks and earthquake swarms. Asperities are shown as contours every 1 m of displacement on the fault for the Tokachi-oki earthquake [*Yamanaka and Kikuchi*, 2003]. (b) Space-time plot of earthquakes shown in Figure 3a. (c) Temporal change in *b*-value and M_C in the whole study area. M_C is the minimum magnitude that satisfies the G-R relation. The time window is two years long. For example, a value plotted for 1995 is calculated from earthquakes between 1994 and 1996. (d) Cumulative number of earthquakes as a function of time. Magnitudes labels on each curve indicate the lower threshold of magnitude. For example, the curve with a label of M4.0 represents the cumulative number of earthquakes with $M \geq 4.0$.

(Figure 3c). Figure 3d plots the cumulative number of events versus time, and it can be seen that the reporting in this catalog does not change with time over the entire magnitude range. In addition, as shown in Figure 4, there is no magnitude shift or stretch during this period. The seismicity rate is almost constant for all magnitude bands and all time windows.

3. Analysis

3.1. ZMAP

[12] The second important requirement for a seismic quiescence analysis is to define the spatiotemporal changes in seismicity quantitatively using statistical parameters. In the present study, a gridding technique (ZMAP) [*Wiemer and Wyss*, 1994] is used to produce an image of the significance of rate changes in space and time. Key parameters for the ZMAP analysis are listed in Table 1. The study area is divided by a grid from 41°N to 44°N and from 141°E to 146°E with an interval of 0.05°. Thus, the total number of nodes is 61 × 101 = 6,161. A circle is drawn around each node and its radius r is increased until it includes a total number of epicenters of $N = 100$. This circle represents the resolution for a given value of N. The radii are variable and are inversely related to the local seismicity rate because N is kept constant to allow statistical comparisons. The cumulative number of events versus time is plotted for each node, starting at a time t_0 (1 January 1994) and ending at a time t_e (25 September 2003). A time window is then placed, starting at T_s and ending at $T_s + T_w$, where $t_0 \leq T_s \leq T_s + T_w \leq t_e$. A T_w value of 4.0 years is used here, and T_s is moved forward in steps of 0.04 years (~14 days). For each window position, the Z-value is calculated, generating the function LTA defined by *Wiemer and Wyss* [1994], which measures the significance of the difference between the mean seismicity rate R_w within the window T_w, and the background rate R_{bg} that is defined here as the mean rate in

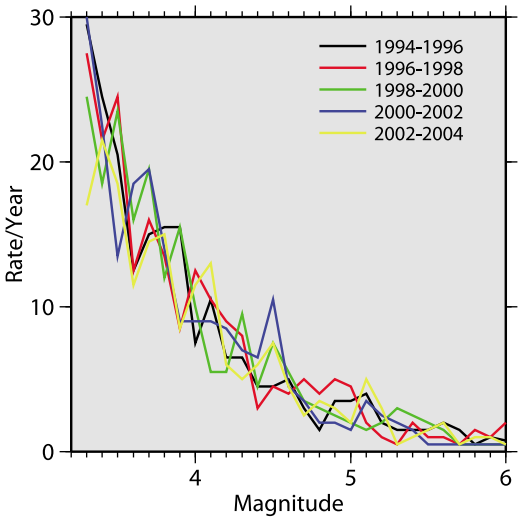

Figure 4. Histogram of seismicity rate for two-year periods.

the time period between t_0 and t_e, excluding T_w. The Z-value is defined as

$$Z = (R_{bg} - R_w)/(S_{bg}/n_{bg} + S_w/n_w)^{1/2}, \quad (1)$$

where S and n are the variance and number of samples, respectively.

[13] An example of a Z-value calculation is as follows. First, the number of earthquakes is counted within a time window called a bin with a length of 14 days. The length of the earthquake catalog is 3,555 days between 1 January 1994 and 25 September 2003. Therefore, the number of bins is 3,555/14 ~ 254. Assuming that the i-th bin includes r_i (i = 1 to 254) events, T_w is set to 4 years from the 100th to the 203rd bin. R_{bg} and R_w are then calculated as follows:

$$R_{bg} = \left(\sum_{i=1}^{99} r_i + \sum_{i=204}^{254} r_i\right)/(99 + 51)$$

$$R_w = \left(\sum_{i=100}^{203} r_i\right)/104$$

The variances S_{bg} and S_w are calculated using

$$S_{bg} = \left\{\sum_{i=1}^{99} (r_i - R_{bg})^2 + \sum_{i=204}^{254} (r_i - R_{bg})^2\right\}/(99 + 51)$$

$$S_w = \left\{\sum_{i=100}^{203} (r_i - R_{bg})^2\right\}/104$$

Finally, the Z-value is calculated from equation (1) using R_{bg}, R_w, S_{bg}, S_w, n_{bg} = 150 and n_w = 104.

[14] The Z-maps shown in Figure 5 present time slices for the re-examined earthquake catalog every one year between T_s = 1995 and 1998. Earthquakes that occurred within the Pacific plate are selected and no declustering process is applied before the calculation of the Z-values. For each time slice, only grid points that have a resolution circle with a radius of less than 60 km are selected and colored; these define the effective grid points. The number of effective grid points is 3,327 for each time slice, and since there are 144 time slices, the total number of effective grid points where Z-values are calculated is 479,088. Among these, only 12 nodes have Z-values larger than +3.9 (Table 2).

[15] Positive Z-values indicate that the seismicity rate is lower than the background rate. Based on the location and starting time, the above 12 nodes are divided into two anomalies: from No. 1 to 4 (Anomaly 1) and from No. 5 to 12 (Anomaly 2). Nodes 1 to 4 are located at (42.3°N, 144.0°E) in the asperity ruptured by the 2003 Tokachi-oki earthquake (A1 in Figure 5). The start time of Anomaly 1 is 1998.820 ± 0.06, obtained by taking the average T_s for nodes 1 to 4. Thus, the duration of the seismic quiescence is 2003.745 - 1998.820 = 4.925 years and its Z-value is +3.9. The spatial extent is defined as the radius of the resolution circle, which is 40 km for Anomaly 1. Nodes 5 to 8 are located at (42.8°N, 144.1°E) and nodes 9 to 12 at (42.9°N, 144.2°E). The distance between these two locations is only 14 km, which is smaller than the resolution circle, so it is assumed that nodes 5 to 12 form a single anomaly. The parameters for Anomaly 2 are represented by the values obtained at node 9: the center of the anomalous area is (42.9°N, 144.2°E), the start time is 1999.520, the duration of the seismic quiescence is 2003.745 – 1999.520 = 4.225 years and the Z-value is +4.0. The radius of the resolution circle is 25 km. Anomaly 2 is located around the northern boundary of the Tokachi-oki asperity and the Z-value determined here is the maximum value obtained in the present study. The obtained parameters of the seismic quiescences are summarized in Table 3.

3.2. Decrease in Stressing Rate

[16] Only five of the epicenters associated with the two anomalies overlap each other, as seen in Figure 6a. Epicenters within Anomaly 1 are located in a relatively deeper portion of the asperity ruptured by the 2003 main shock, and hence the rupture initiation point is located in a non-quiescent volume. This is consistent with the results of some previous studies [*Wyss*, 1986, Figure 9; *Wyss and Habermann*, 1988]. On the other hand, epicenters within Anomaly 2 are distributed at the northern boundary of the asperity. All earthquakes used in this study are located on the upper boundary of the Pacific plate or within the Pacific plate. Therefore, the quiescent volumes are included in the footwall of the seismic fault ruptured by the 2003 main shock.

Table 1. Characteristic Parameters for ZMAP in This Study

Parameter	Value
Study area	141.0–146.0°E, 41–44°N
Time interval of earthquake catalog	1 January 1994–25 September 2003
Time length of earthquake catalog (days)	3555
Magnitude range	M ≥ 3.3
Depth range of hypocenters (km)	0–200
The total number of earthquakes	2000
Grid interval	0.05° × 0.05°
Radius of resolution circles (km)	r ≤ 60
The number of effective grids	3327
Length of bin (days)	14
Time step of T_s (years)	0.04
The number of time steps	144
The number of earthquakes for each grid	100
T_w (years)	4.0

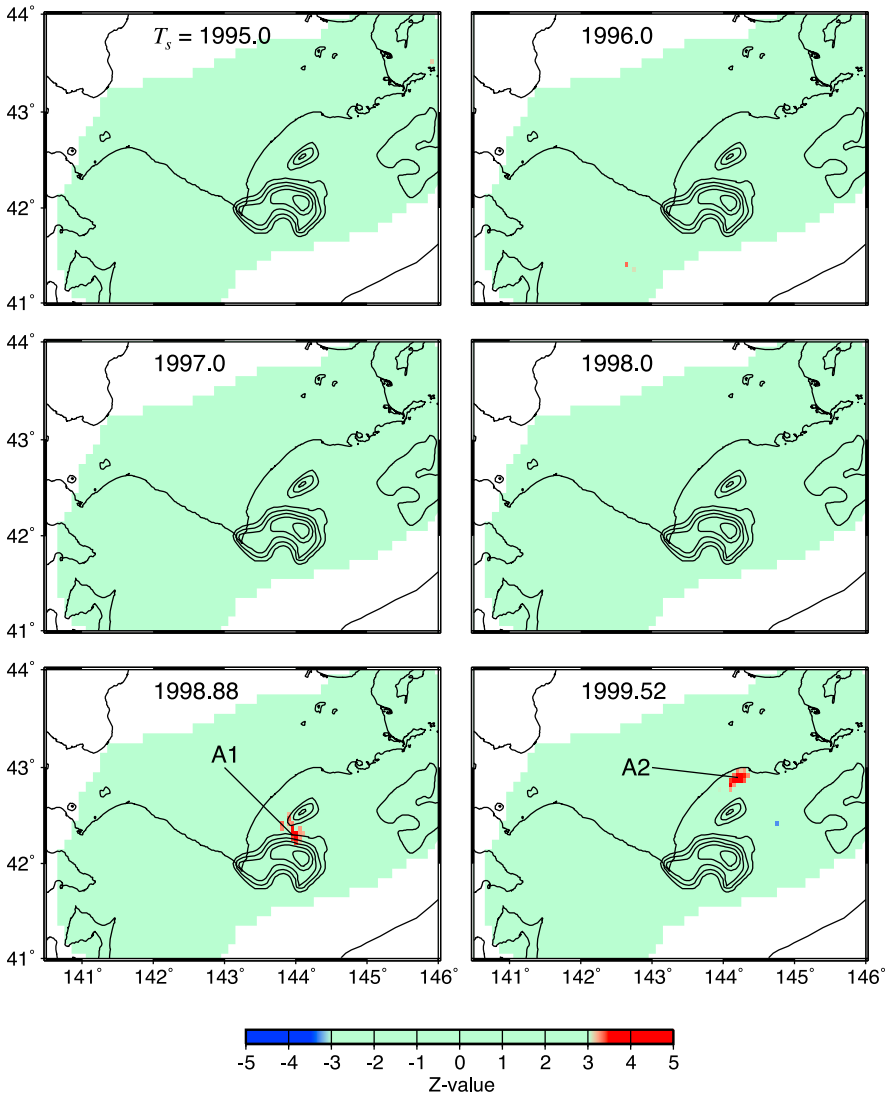

Figure 5. Time slices of Z-value distribution using the re-examined non-declustered catalog. The time window starts at T_s and ends at $T_s + T_w$, where $T_w = 4$ years. Only grid points with a radius of the resolution circle smaller than 60 km are selected. The number of such points is 3327. A red color (positive Z-value) and blue color (negative Z-value) represent a decrease and increase in the seismicity rate, respectively. Two alarms with Z-values larger than +3.9 are detected: A1 and A2 (see text). Asperities are shown as contours every 1 m of displacement on the faults for the Tokachi-oki and the Nemuro-oki earthquakes [*Yamanaka and Kikuchi*, 2003].

[17] To verify the reliability of the seismicity rate changes determined in the previous section, the cumulative number of earthquakes is examined as a function of time in those volumes. The cumulative curves in Figure 6 indicate seismicity rate changes at specific nodes in the cases of Anomalies 1 and 2. The statistical functions, LTA, displayed in Figure 6 are the Z-values calculated by the method described in Section 3.1. Since a peak in Z-value corresponds to the time when the change in the seismicity rate starts, both of the clear anomalies are found to start around the beginning of 1999 and persist until the main shock in September 2003. The seismicity rate clearly decreases from 12.4 to 7.2 events/year (a drop of 42%) for Anomaly 1 and from 11.9 to 6.1 events/year (a drop of 49%) for Anomaly 2. Anomaly 1 exhibits almost the same seismicity rate as Anomaly 2 both before and after the start of the seismic

Table 2. Large Z-values Obtained by ZMAP Analysis[a]

	Longitude	Latitude	*Ts*	*r*	*Z*
1	144.00	42.30	1998.76	40.4	3.9
2	144.00	42.30	1998.80	40.4	3.9
3	144.00	42.30	1998.84	40.4	3.9
4	144.00	42.30	1998.88	40.4	3.9
5	144.10	42.80	1999.52	25.3	3.9
6	144.10	42.80	1999.56	25.3	3.9
7	144.10	42.80	1999.60	25.3	3.9
8	144.10	42.80	1999.64	25.3	3.9
9	144.20	42.90	1999.52	25.1	4.0
10	144.20	42.90	1999.56	25.1	3.9
11	144.20	42.90	1999.60	25.1	3.9
12	144.20	42.90	1999.64	25.1	3.9

[a] T_s, the time that the seismic quiescence started; r, radius of resolution circle in km; Z, Z-value, positive and negative values indicate decrease and increase in seismicity rate, respectively.

Table 3. Parameters of Precursory Quiescences to the M_w = 8.3 Tokachi-oki 2003 Earthquake

Anomaly	Sample Size, N	Window Length, T_w(years)	Relative Significance, Z	Start Date, T_s	Duration (years)	Radius of Resolution Circle, r (km)
1	100	4	3.9	1998.82	4.9	40
2	100	4	4.0	1999.52	4.2	25

quiescence. Since the onset time of quiescence is sharply defined, its duration is well defined. Anomaly 2 includes aftershocks following the M_w = 7.6 Kushiro-oki earthquake in January 1993 [*Ide and Takeo*, 1996]. This earthquake ruptured a near-horizontal fault within the Pacific plate at a depth of 100 km. The term "aftershocks" is probably misleading because the rate of aftershock occurrence usually decreases as a function of time. In the case of the 1993 Kushiro-oki earthquake, the earthquake rate decreased very rapidly until the end of 1993. However, after that it became almost constant. The

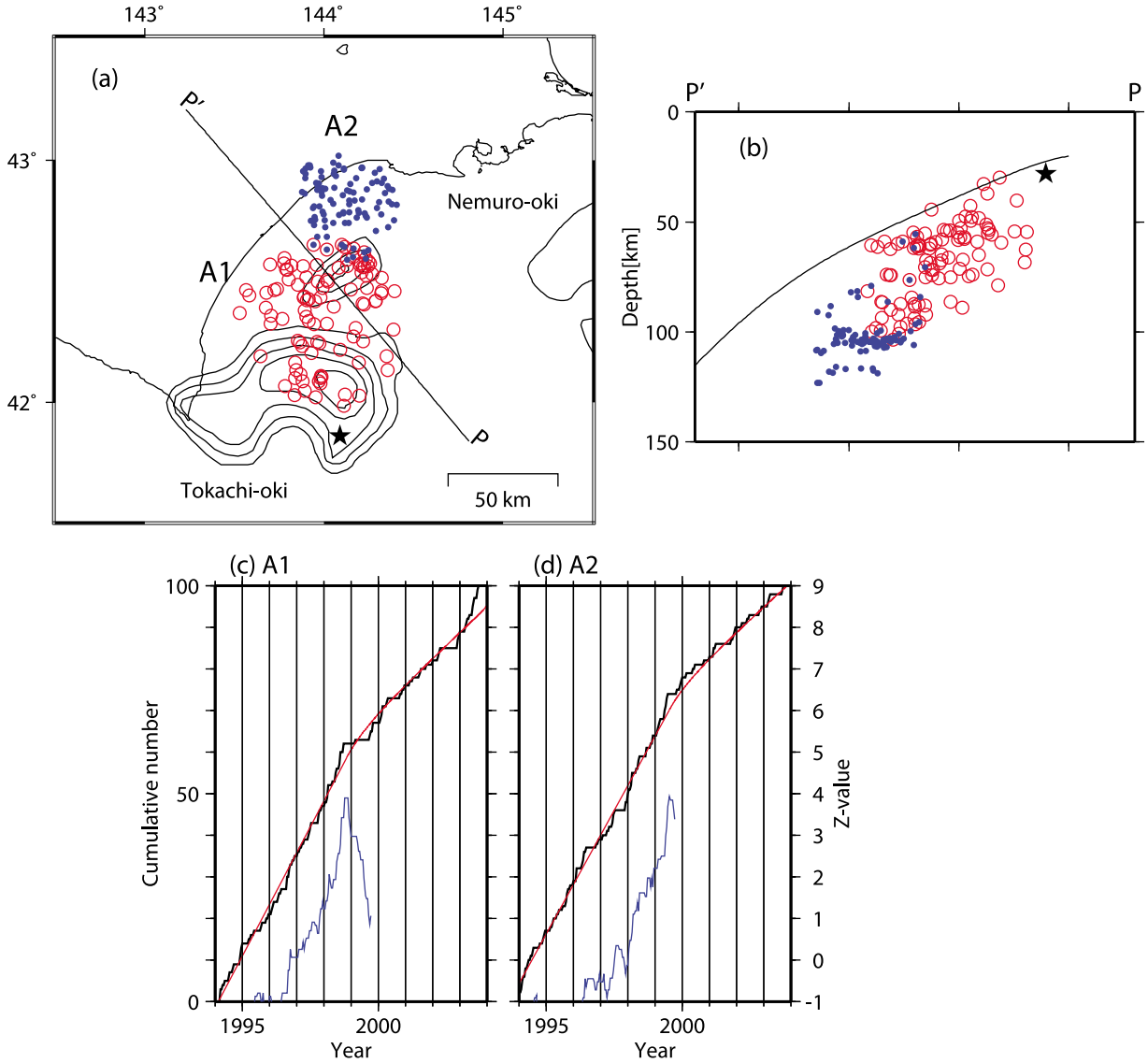

Figure 6. Cumulative number and Z-value plots for anomalous areas detected in Figure 5. (a) Distribution of epicenters in the areas of Anomaly 1 (A1, red open circles) and Anomaly 2 (A2, closed blue circles). The star indicates the epicenter of the main shock. Asperities are shown as contours every 1 m of displacement on the faults for the Tokachi-oki and the Nemuro-oki earthquakes [*Yamanaka and Kikuchi*, 2003]. (b) Vertical cross section along P-P′ in Figure 6a with the upper boundary of the Pacific plate determined by *Katsumata et al.* [2003]. (c and d) show the cumulative number (black line), the Z-value (blue line), and a theoretical curve for the cumulative number calculated from equation (2), assuming that the stressing rate ratio is 0.5 (red line).

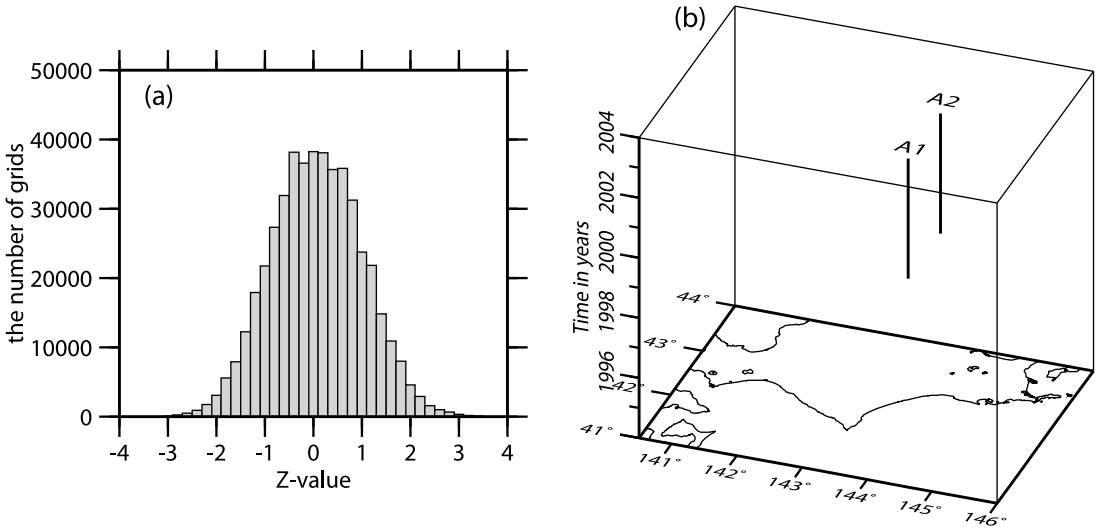

Figure 7. (a) *Z*-value distribution. The number of grid points scanned is 475,761 in the alarm cube for the ISV non-declustered catalog. (b) Alarm cube. Vertical bold lines with a time length of 4 years indicate alarms with *Z*-values larger than +3.9. Only two alarms are detected: A1 and A2 indicate the quiescence.

cumulative curve in Figure 6d is clearly a straight line between 1994 and 1999 rather than the convex curve usually associated with aftershock activity. It is for this reason that the aftershocks of the Kushiro-oki earthquake were not removed from the catalog.

[18] Dieterich's seismicity rate theory [*Dieterich*, 1994] is used to relate the stressing rate and the seismicity. Suppose that the stressing rates are $\dot{\tau}_r$ before time T_0, $\dot{\tau}$ between times T_0 and T_1, and again $\dot{\tau}_r$ after time T_1. Then, the following equation gives the cumulative number of earthquakes at time t:

$$N(t) = rt_a \ln\left[\frac{\dot{\tau}_r}{\dot{\tau}}\left(\exp\left(\frac{\dot{\tau}(t-T_0)}{\dot{\tau}_r t_a}\right)-1\right)+1\right] \text{for } T_0 < t < T_1, \tag{2}$$

where r and t_a are the background seismicity rate per year and the aftershock decay time in years, respectively [*Segall et al.*, 2006; *Aoi et al.*, 2010]. The ratio $\dot{\tau}/\dot{\tau}_r$ of the stressing rates is then calculated under the assumption that the seismic quiescence anomalies are caused by a change in the stressing rate. The times T_0 and T_1 are assumed to be the start time of the quiescence anomaly and the origin time of the 2003 main shock, respectively. The background seismicity rate is assumed to be the mean rate between 1 January 1994 and time T_0. The ratio $\dot{\tau}/\dot{\tau}_r$ determines the slope of the cumulative curve during the seismic quiescence, and t_a determines how fast the seismicity rate changes when the seismic quiescence starts. Since the seismic quiescences start suddenly rather than gradually in this case, t_a is expected to be small. A grid search is then performed for t_a and $\dot{\tau}/\dot{\tau}_r$, where it is assumed that t_a and $\dot{\tau}/\dot{\tau}_r$ are the same for Anomalies 1 and 2. T_0 and r are 1998.820 and 12.4 events/year in the case of Anomaly 1, and 1999.520 and 11.9 events/year in the case of Anomaly 2. Three pairs, (t_a, $\dot{\tau}/\dot{\tau}_r$) = (0.7, 0.4), (0.5, 0.5) and (0.3, 0.6) are found to produce good agreement between the observed and the synthetic curves (Figure 6). Interestingly, the results suggest that the stressing rate in the period of seismic quiescence is half of the ordinary background rate for both Anomalies 1 and 2. The duration of aftershock activity is usually very short for small earthquakes within the Pacific plate in this region, which is consistent with the value t_a = 0.3–0.7 years obtained in the present study. The red lines in Figures 6c and 6d for the time period 1 January 1994 to T_0 are linear fits to the cumulative number of earthquakes versus time (i.e., the slope of these lines is the background seismicity rate before T_0).

3.3. Alarm Cube

[19] The two anomalies mapped in Figure 5 and characterized in Figure 6, associated with the Tokachi-oki main shock, may have no particular significance if similar anomalies occur frequently at locations in space and time where no main shocks occur. Figure 7a shows a histogram of *Z*-values calculated at all the nodes; it indicates that few *Z*-values larger than +3.0 or smaller than −3.0 are observed in this case. As mentioned in the previous section, the *Z*-value is calculated at 479088 nodes and *Z*-values larger than +3.9 are found at only 12 nodes, that is, the probability is only 12/479088 = 0.0025%. Another method of displaying *Z*-value anomalies that could be false alarms is by the use of alarm cubes [*Wiemer*, 1996; *Wyss et al.*, 1996; *Wyss and Martirosyan*, 1998]. In these three-dimensional figures (Figure 7b), the horizontal axes are the spatial coordinates in the study area and the vertical axis is time. Anomalies are defined as instances of *Z*-values larger than +3.9 at any node and any time. Figure 7b illustrates visually that the results are reliable. As listed in Table 2, the alarm cube includes two outstanding anomalies starting around January 1999.

[20] The alarm distribution as a function of N and T_w is shown in Figure 8. The *Z*-values corresponding to Anomaly 1 range from 2.9 to 3.9 when the sample size N and the time window T_w are 90 to 110 and 3.5 to 4.5 years, respectively. On the other hand, Anomaly 2 always has *Z*-values above 3.8 regardless of N and T_w. Therefore, the Tokachi-oki quiescence anomalies are most strongly developed in data sets with N = 100 and T_w = 4.0 years (Figure 5 and Table 2) and these quiescences are also unique (no other data sample produces a *Z*-value equal to or larger than that associated with the Tokachi-oki quiescence anomalies).

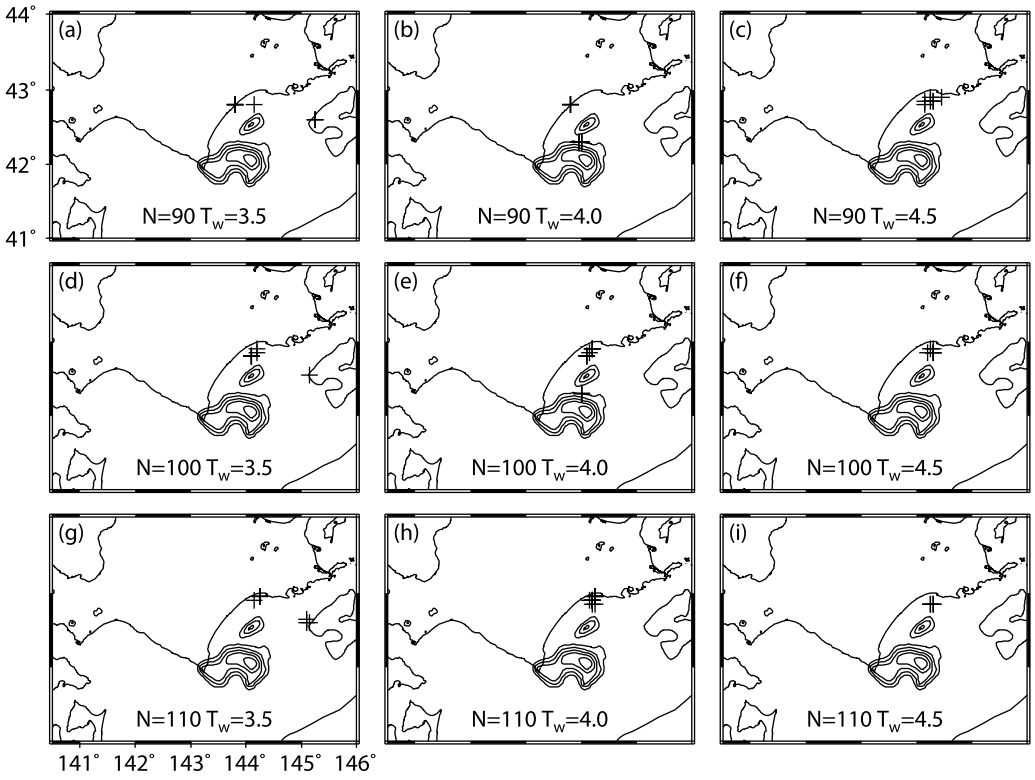

Figure 8. Alarm distribution as a function of N and T_w. Only alarms with a Z-value of 3.8 or larger are plotted by crosses. For each line N is constant, starting with $N = 90$ at the top and ending with $N = 110$ at the bottom. T_w is constant for each column, starting with 3.5 years at the left and ending with 4.5 years at the right. Only grid points with a radius of the resolution circle smaller than 60 km are selected. Asperities are shown as contours every 1 m of displacement on the faults for the Tokachi-oki and the Nemuro-oki earthquakes [*Yamanaka and Kikuchi*, 2003].

3.4. Probable Magnitude Changes

[21] Since an apparent seismicity change is often due to man-made causes, the Z-value anomalies found in the present study should be carefully examined. In particular, magnitude shifts and stretches critically affect the results [*Wiemer and Wyss*, 1994]. Figure 9 shows magnitude signatures for the whole study area for two time windows, before and after 1999.5 (1 July 1999), which is around the start time of the two anomalies. The b-values in the magnitude-frequency plot are 0.68 and 0.70 before and after the start time, respectively, which are almost identical (Figure 9a). In addition, the seismicity rate shows no change for $M \geq 3.3$ (Figures 9b and 9c). From this, it can be concluded that there is no significant magnitude shift or stretch in the whole study area before or after the start time of the Z-value anomalies.

[22] Figure 10 shows magnitude signatures for Anomalies 1 and 2 for two time windows, before and after the start time of the anomalies. In these plots, all earthquakes with $M \geq 3.0$ are considered. For Anomaly 1, the b-value decreases from 0.91 to 0.61. This is due to a decrease in the number of earthquakes smaller than $M = 4.0$ and an increase in the number of those larger than $M = 4.0$. It is unlikely that there is a man-made shift in the magnitude-frequency distribution because there is no change in the detection capability or b-value over the whole study area, as shown in Figure 9. In addition, *Nakaya* [2006] found a spatiotemporal variation in the b-value within the subducting slab prior to the 2003 Tokachi-oki earthquake, based on an earthquake catalog produced by JMA, which is consistent with the decrease in b-value detected in this study. This decrease seems to be another precursor to the main shock, but this is outside the scope of the present study. Therefore, it can be concluded that Anomaly 1 is not a man-made effect. For Anomaly 2, the b-values are similar in the two time windows: $b = 0.80$ and 0.70 before and after the start of quiescence, respectively. The number of earthquakes decreases for all magnitudes $M > 3.0$. Therefore, it can also be concluded that this quiescence is not a man-made artifact.

3.5. Statistical Significance of the Results

[23] In order to estimate the statistical significance of the Z-value anomalies detected in this study, synthetic seismicity data is generated, and Z-value matrices and the distribution of maximum Z-values, Z_{max}, are determined. First, a single day is extracted at random from the 3,555 days between 1 January 1994 and 25 September 2003 and repeated it $N = 2{,}000$ times to produce a synthetic earthquake catalog with 2,000 earthquakes. In this process, the UNIX command "rand()" is used to produce an integer between 1 and 3,555 and the seed is initialized by the command of "srand(usec)," where usec is the internal clock time in microseconds. Latitudes and longitudes of epicenters are also assigned randomly to the 2,000 earthquakes. This synthetic seismicity data are assigned to a rectangular area from 41°N to 44°N and from 142°E to 145°E. In

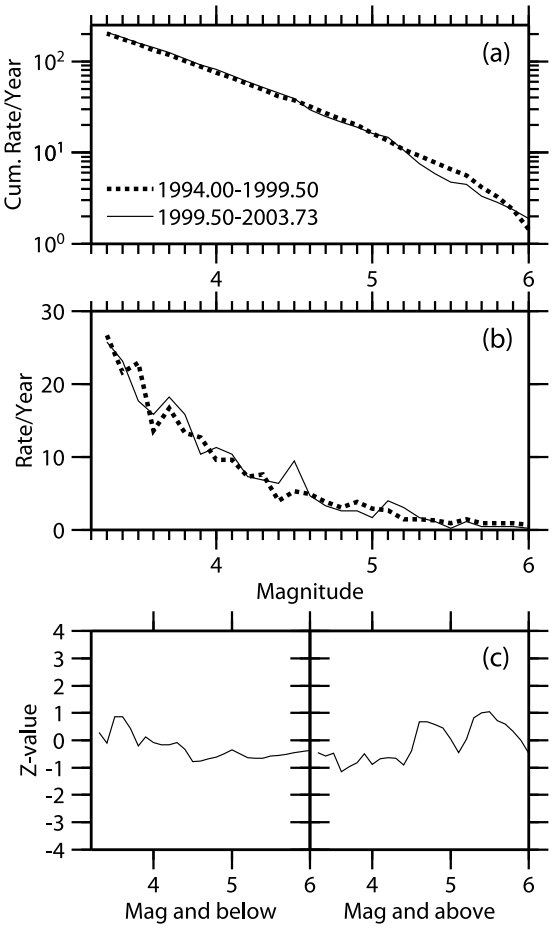

Figure 9. Magnitude signatures for the whole study area. Broken and bold lines indicate the normal period (1994.00–1999.50) and the anomalous period (1999.50–2003.73), respectively. (a) Plot of magnitude versus cumulative number. (b) Plot of magnitude versus frequency. (c) Plot of magnitude versus *Z*-value. The label "Mag and below" on the horizontal axis in Figure 9c means that the *Z*-values are calculated for earthquakes with a magnitude equal to or less than the values indicated on the axis scale.

this area, 300 nodes are distributed in latitude with an interval of 0.01° and one node is extracted randomly by producing an integer from 1 to 300. In the same manner a longitude is assigned independently. By using these 2,000 synthetic earthquakes, the *Z*-values are calculated at all nodes with an interval of 0.05° in latitude × 0.05° in longitude in the simulation area. Thus, the number of nodes is 3,600, which is almost the same as the value of 3,327 used in the real study area. Other parameters for the *Z*-value calculation are assumed to be same as for the real analysis in this study: the cumulative number of earthquakes is 100, the time window T_w is 4 years, the bin length is 14 days, and the time step of T_s is 0.04 years. The algorithm for calculating the *Z*-values is also the same as that described in section 3.1.

[24] This procedure is repeated 5,000 times and Z_{max} is evaluated for each repetition. The resulting Z_{max} distribution is shown in Figure 11a; Z_{max} is seen to range from 3.01 to 6.03 and the average is 4.20. Based on this distribution, the probability of Z_{max} being 3.9 or larger is 74%, and the probability of it being 4.0 or larger is 65%. Therefore, neither of the two anomalies detected in this study is a rare phenomenon. In other words, if earthquake observations are performed for about 15 years in the study area, a seismic quiescence characterized by a *Z*-value of 3.9 will be detected at least once.

[25] However, it may still be considered unlikely that two such anomalies would occur at almost the same time. The onset times of Anomalies 1 and 2 are 1998.82 and 1999.52, respectively, which is a difference of only 0.7 years. Moreover, the resolution circles for the two anomalies are not overlapping (Figure 6a). Anomaly groups that satisfy the two conditions are counted: (1) $Z \geq 3.9$ and (2) the difference of the start time is less than 0.7 years. I find that the probability that two such anomalies occur by chance is 12% (Figure 11b). Since the time period of the earthquake catalog used in this study is approximately 10 years, this probability suggests that this phenomenon occurs once every ~80 years. Interestingly, this is almost the same as the recurrence interval of the Tokachi-oki earthquake. Based on the results of the numerical simulations, two different models can be proposed: (1) Non-precursor model: the seismic quiescence detected in this study started by chance five years before a great earthquake which has repeated every 50 years, and (2) the Precursor model: seismic quiescences similar to those detected in this study occurred every 50 years as precursors to great earthquakes. Although the anomalies detected in this study are not statistically significant, the Precursor model would appear to be more plausible in view of the physical cycle associated with the subduction of the Pacific plate. Similar analyses at other subduction zones would help to clarify the background physics of spatiotemporal changes in seismicity.

3.6. A Quasi-Static Slip Model

[26] Whereas some possible mechanisms causing precursory quiescence have been proposed, such as strain softening [*Stuart*, 1979] and dilatancy hardening [*Scholz*, 1988], the most plausible model would be slow propagation of slip along a fault. This hypothesis is also supported by other observations and numerical simulations. Based on an analysis of small repeating earthquakes, *Uchida et al.* [2009] found that the rate of quasi-static slip on the upper boundary of the Pacific plate increased in the area to the northeast of the asperity ruptured by the 2003 Tokachi-oki earthquake (around Region F in Figure 3b of *Uchida et al.* [2009]). The location of the quiescence anomalies in Figure 6 agrees with that of Region F of *Uchida et al.* [2009]. They also found that the increased slip rate persisted for 3 years before the 2003 Tokachi-oki earthquake. This is shorter than the values of 4.2–4.9 years estimated for Anomalies 1 and 2 in this paper. However, the increase in slip rate seems to have started in the middle of 1999 [*Uchida et al.*, 2009]. In this case, the duration is longer than 4 years, which is consistent with the duration of the seismic quiescence. They suggested that the behavior in Region F is probably peculiar to the transition zone between strongly locked (coseismic slip) and stably slipping areas. Based on an analysis of GPS data, *Baba and Hori* [2006] suggested that the deeper half of the plate interface, within the rupture area of the 2003 Tokachi-oki earthquake, became uncoupled several years prior to the main shock. Based on changes in the seismicity rate in regions far from the 2003 Tokachi-oki area, *Ogata* [2005] pointed out that a slow slip event occurred on a deeper

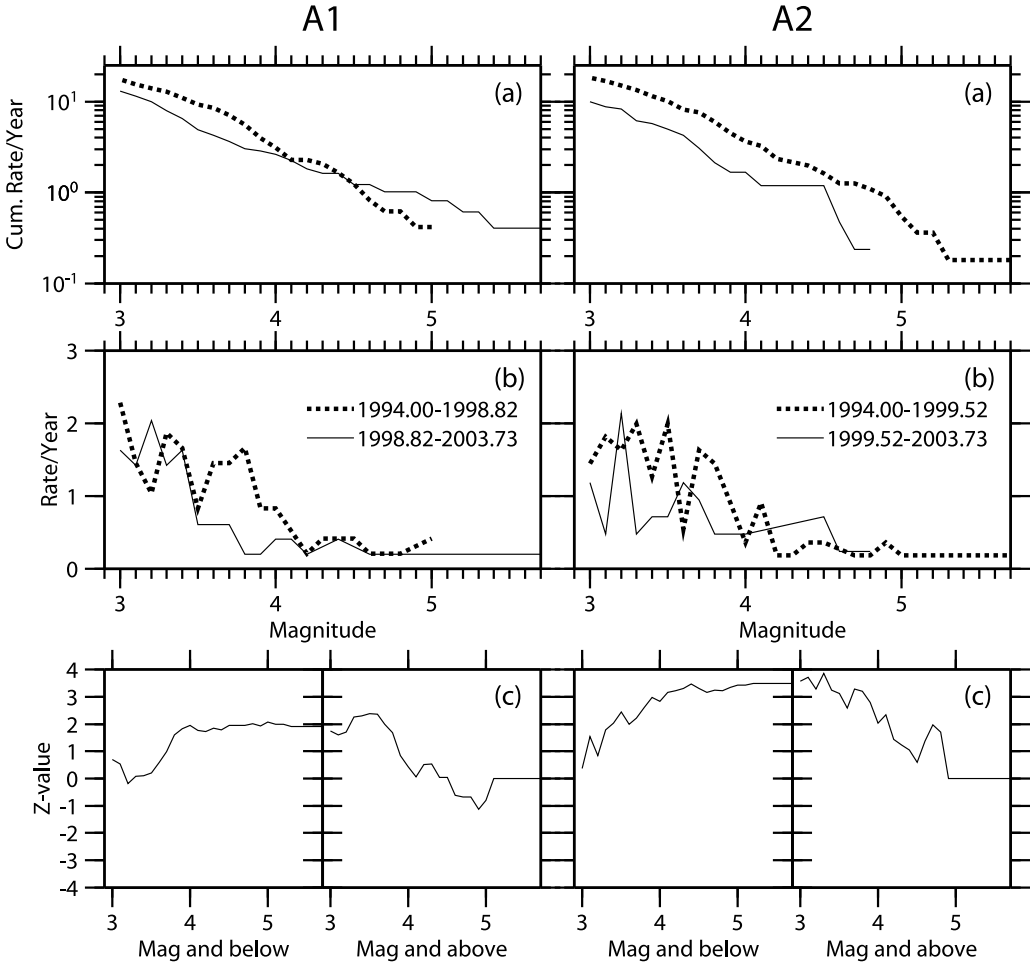

Figure 10. Magnitude signatures for the two anomaly areas: A1 and A2. Broken and bold lines indicate the normal period and the anomalous period, respectively. (a) Plot of magnitude versus cumulative number. (b) Plot of magnitude versus frequency. (c) Plot of magnitude versus *Z*-value. The label "Mag and below" on the horizontal axis in Figure 10c means that the *Z*-values are calculated for earthquakes with a magnitude equal to or less than the values indicated on the axis scale.

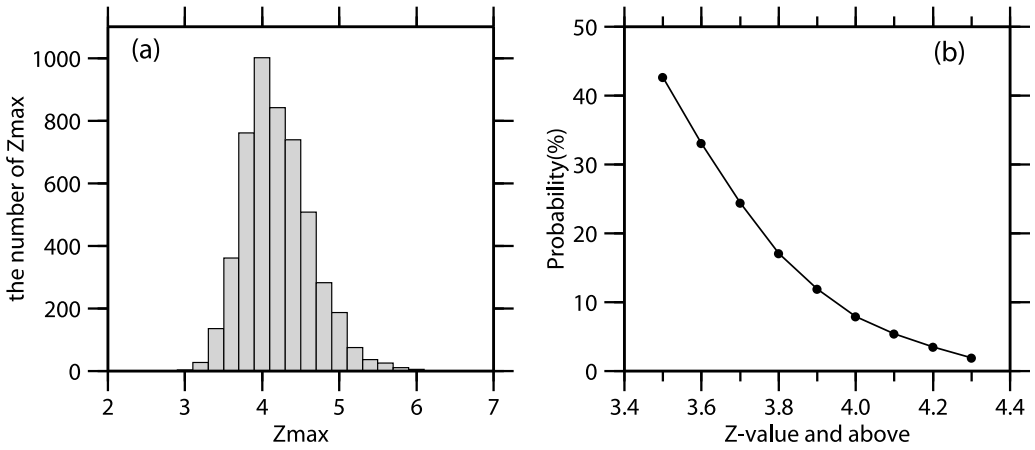

Figure 11. Numerical simulations assuming that earthquakes occur randomly in space and time. 5,000 synthetic earthquake catalogs are produced by UNIX commands. (a) Distribution of Z_{max}, obtained by the same ZMAP analysis that is applied to the real earthquake catalog. (b) Probability of detection of two spatially separate quiescences with a time difference of less than 0.7 years. The label "Z-value and above" on the horizontal axis means that the two anomalies have *Z*-values equal to or larger than the values indicated on the axis scale.

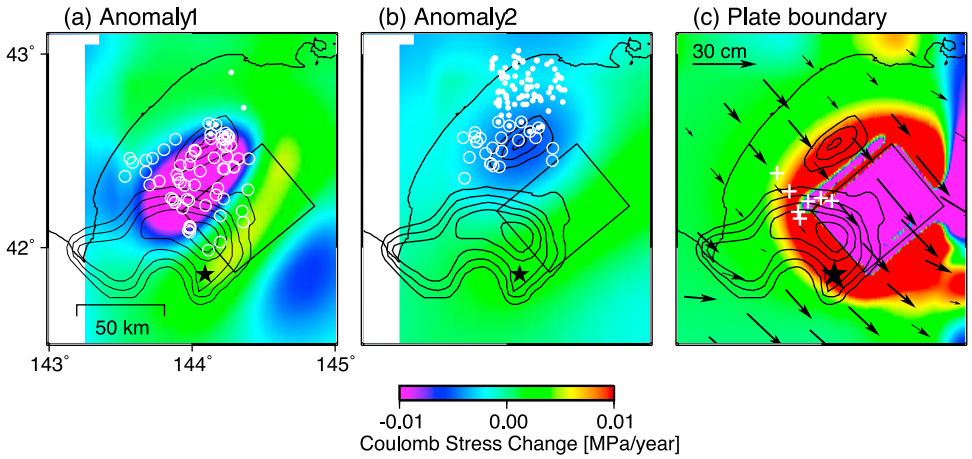

Figure 12. Change in Coulomb failure stress (ΔCFS) in and around the quiescence anomalies. Open and closed white circles indicate the epicenters included in the volume of Anomalies 1 and 2, respectively. (a) ΔCFS at a depth of 65 km. Epicenters at depths from 50 to 80 km are plotted. The focal mechanism of receiver earthquakes is assumed to be the downdip-extension type: strike = 40°, dip = 80°, and slip = 60°. (b) ΔCFS at a depth of 100 km. Epicenters at depths from 80 to 110 km are plotted. The focal mechanism of receiver earthquakes is assumed to be the downdip-extension type: strike = 136°, dip = 11°, and slip = −30°. (c) ΔCFS on the plate boundary. The black star shows a hypocenter of the 2003 Tokachi-oki main shock determined by ISV, and asperities are shown as contours every 1 m of displacement on the fault determined by *Yamanaka and Kikuchi* [2003]. Arrows indicate the afterslip from 2 October 2003 to 10 November 2003 determined by *Ozawa et al.* [2004]. Crosses indicate epicenters of the small repeating earthquakes in Region F in Figure 3b of *Uchida et al.* [2009]. The focal mechanism of receiver earthquakes is assumed to be same as the Tokachi-oki main shock determined by *Yamanaka and Kikuchi* [2003]: strike = 230°, dip = 20°, and slip = 109°. The rectangle is a projection onto the ground surface of an assumed fault plane of a quasi-static slip with length = 60 km and width = 50 km, which is located on the upper boundary of the Pacific plate. The southwestern point of the fault plane is located at 144.30°E, 41.87°N, and depth = 20 km. The fault parameters are assumed to be the same as those for the Tokachi-oki main shock determined by *Yamanaka and Kikuchi* [2003]: strike = 230°, dip = 20°, and slip = 109°. The displacement is assumed to be 3 cm/year, which is the slip velocity required to build up a seismic moment corresponding to M_w = 6.0 over five years. The displacement of the ground surface caused by a M_w = 6.0 quasi-static slip is too small to detect even if a dense GPS network is deployed on land.

extension of the seismic fault ruptured by the 2003 main shock. *Katsumata et al.* [2002] presented a quasi-static slip model for explaining anomalies recorded by tide gauges before the 1994 *Mw* = 8.3 Hokkaido-Toho-oki earthquake. Recent simulations based on a laboratory-derived friction law [*Kato et al.*, 1997; *Kato*, 2003; *Yoshida and Kato*, 2003] showed that a future fault plane can generate a quasi-static slip starting several years prior to a main shock.

[27] To test the quasi-static slip model, the Coulomb failure stress change (ΔCFS) in and around the quiescence anomaly areas is calculated. In its simplest form, ΔCFS is defined by:

$$\Delta CFS = \Delta\tau + \mu\Delta\sigma_n$$

where $\Delta\tau$ is the shear stress change on a fault and $\Delta\sigma_n$ is the normal stress change. μ is the effective friction coefficient (with a range of 0–1). Failure is encouraged if ΔCFS is positive and discouraged if negative [e.g., *Stein and Lisowski*, 1983; *Stein*, 1999]. $\Delta\tau$ and $\Delta\sigma_n$ are calculated in an elastic half-space based on *Okada* [1992] assuming that the shear modulus is 3.0×10^{10} N/m^2 and the Poisson's ratio is 0.25. The effective friction coefficient is taken to be 0.4. A rectangular fault plane for the quasi-static slip is assumed to be located on the upper boundary of the subducting Pacific plate. The fault parameters are the same as those for the 2003 Tokachi-oki main shock determined by *Yamanaka and Kikuchi* [2003]: strike = 230°, dip = 20°, and slip = 109°. Based on the analysis of the cumulative number curves in the previous section, the stressing rate was found to be half the background rate in the quiescence period. Thus, it is reasonable to assume that the backslip rate on the plate boundary was half of the ordinary averaged rate. The average co-seismic displacement was 2.6 m on the 90 km × 70 km fault plane ruptured by the 2003 main shock [*Yamanaka and Kikuchi*, 2003]. Since the previous Tokachi-oki earthquake occurred in 1952, the mean backslip rate is ~5 cm/year for 51 years. Therefore, ΔCFS is calculated by assuming that the slip velocity is 3 cm/year for the quasi-static slip, and that the slip lasts for five years. The optimal size and location of the fault plane are searched for using a trial-and-error method to match the quiescence anomaly areas to the negative ΔCFS areas. In calculating the spatial pattern of ΔCFS, suitable focal mechanisms should be assumed for receiver earthquakes. In

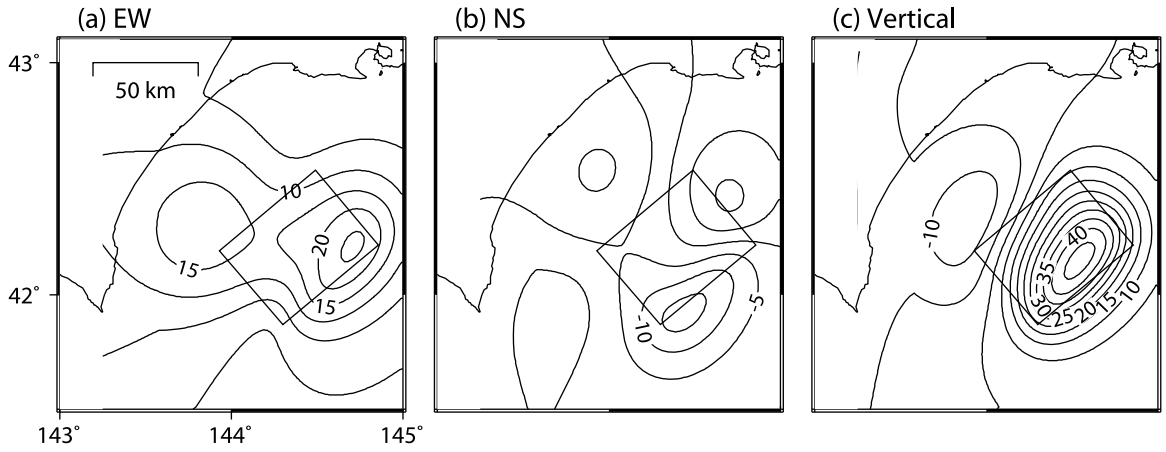

Figure 13. Five-year displacement of the ground surface in mm. (a) East-West, (b) North-South, and (c) vertical components. Contours are shown every 5 mm. The rectangle is a projection onto the ground surface of an assumed fault plane of a quasi-static slip with length = 60 km and width = 50 km, which is located on the upper boundary of the Pacific plate. The southwestern point of the fault plane is located at 144.30°E, 41.87°N, and depth = 20 km. The fault parameters are assumed to be same as those for the Tokachi-oki main shock determined by *Yamanaka and Kikuchi* [2003]: strike = 230°, dip = 20°, and slip = 109°. The displacement is assumed to be 150 mm (= 30 mm/year × 5 years), which is the slip corresponding to M_w = 6.0.

this study, the receivers are the earthquakes included in the volumes of Anomalies 1 and 2. The National Research Institute for Earth Science and Disaster Prevention (NIED) publishes a catalog of focal mechanism solutions [*Fukuyama et al.*, 1998] determined by the broadband seismograph network, F-net. Based on the NIED catalog, two types of focal mechanisms are dominant in the volume of Anomaly 1: downdip-extension type and plate-boundary type. Although the fault parameters fluctuate slightly, the *T*-axes rather than the *P*-axes of almost all intraplate earthquakes are consistent with the downdip direction of the subducting Pacific plate. Thus, it can be assumed that few earthquakes have a downdip-compression type focal mechanism within the Pacific plate in the volume of Anomaly 1. The representative fault parameters for the downdip-extension type receivers are: strike = 40°, dip = 80°, and slip = 60°. For a receiver on the plate boundary, the same parameters as those for the 2003 Tokachi-oki earthquake are assumed: strike = 230°, dip = 20°, and slip = 109°. Since almost all earthquakes in Anomaly 2 occur in the aftershock area of the 1993 M_w = 7.6 Kushiro-oki earthquake, the same focal mechanism as that for the main shock is assumed in the volume of Anomaly 2: strike = 136°, dip = 11°, and slip = −30° [*Ide and Takeo*, 1996].

[28] The resultant ΔCFS patterns in and around the quiescence anomalies are shown in Figure 12. In the volumes of Anomalies 1 and 2, ΔCFS are ranging from −0.02 to −0.01 MPa/year and from −0.005 to −0.003 MPa/year, respectively. In this study, the effective friction coefficient μ is assumed to be 0.4. This parameter has significant uncertainties [e.g., *Parsons et al.*, 2008; *Aoi et al.*, 2010] and has a strong influence on ΔCFS. In fact, the absolute values of ΔCFS vary by a factor of 3 to 4 if μ changes from 0.0 to 1.0. However, the areas of positive and negative ΔCFS exhibit a stable pattern in space. In this study, it is more important to determine whether areas of negative ΔCFS and the seismic quiescence areas match well, rather than accurately estimating the absolute value of ΔCFS. The size of the fault plane of the quasi-static slip is estimated to be 60 km × 50 km, and the fault plane is located around the northeastern edge of the large asperity ruptured by the 2003 main shock. The fault plane obtained here is clearly smaller than the asperity. A displacement of 15 cm (3 cm/year × 5 years) on the 60 km × 50 km fault plane corresponds to M_w = 6.0, which is too small to allow the GPS stations (GEONET) on land to detect the pre-slip (Figure 13). The deformation on the ground surface is approximately 1 cm at most for five years, and this places a constraint on the maximum size of the fault plane. The fault plane is located at the same depth as the asperity rather than at its deeper extension. A quasi-static slip at the deeper extension of the asperity would not produce a negative ΔCFS around a depth of 65 km within the Pacific plate if a downdip-extension type focal mechanism is assumed for the receiver earthquakes. Thus, it does not well explain the seismic quiescence of Anomaly 1. On the other hand, if a plate-boundary type focal mechanism is assumed for the receiver earthquakes, ΔCFS is positive and the seismicity rate is expected to increase on the plate interface around the fault plane of the quasi-static slip (Figure 12c). Actually the number of small repeating earthquakes increased in Region F in Figure 3b of *Uchida et al.* [2009]. The hypocenter, that is, the rupture initiation point of the 2003 Tokachi-oki main shock, is located in an area with a positive ΔCFS of +0.1 MPa (0.02 MPa/year × 5 years). An increase of 0.1 MPa is not so small, suggesting that the quasi-static slip may have promoted the rupture initiation of the 2003 Tokachi-oki main shock. In the volume of Anomaly 1, the seismicity possibly decreases within the Pacific plate and simultaneously increases at the plate interface. However, the decrease dominates, and thus the quiescence is observed. Interestingly, the fault plane of the quasi-static pre-slip corresponds well to an afterslip area with a slip of ~30 cm from 2 October 2003 to 10 November 2003 [*Ozawa et al.*, 2004]. The afterslip occurred in the area surrounding the main asperity; in particular, the slip seemed to be largest on the pre-slip fault plane. Recent numerical simulations predicted not only a

precursory slip but also afterslips [*Kato et al.*, 1997; *Kato*, 2003; *Yoshida and Kato*, 2003]. Therefore, the sequence "quasi-static slip, main shock and afterslip" constitutes a scenario best suited to the present analysis.

4. Discussion

[29] The earthquake catalog used in this study is of unusually high quality from the point of view of homogeneous reporting in the Hokkaido area (Figure 1). In general, earthquake catalogs are not homogeneous temporally and spatially [*Habermann*, 1987, 1991]. Therefore, as described in section 2, the catalog is carefully re-examined before performing a statistical analysis of long-term seismicity changes. The results indicate a seismic quiescence in and around the asperity ruptured by the 2003 Tokachi-oki main shock. This is the first case study revealing a reliable relationship between such a seismic quiescence area and a ruptured asperity for a subduction earthquake greater than $M = 8$.

4.1. Significance of Rate Decrease

[30] The size of the rate decrease is estimated using the Z-value, and Z-values of +3.9 and +4.0 are found for Anomaly 1 and Anomaly 2, respectively. As shown in section 3.5, a value of Z~4.0 is too small to reject the possibility of a chance coincidence between the seismic quiescence and the 2003 Tokachi-oki earthquake. However, several previous studies have identified seismic quiescences with Z~4.0 that were followed by great earthquakes in subduction zones: $Z = 4.1$ for the Kermadec earthquake ($M_w = 7.9$) in 1976 [*Wyss et al.*, 1984], $Z = 4.4$ for the Tokachi-oki earthquake ($M = 7.9$) in 1968 [*Wyss and Habermann*, 1988], and $Z = 4.0$ for the Hokkaido-Toho-oki earthquake ($M_w = 8.3$) in 1994 [*Katsumata and Kasahara*, 1999]. These results suggest the possibly that even if a seismic quiescence occurs before a great earthquake as an intermediate-term precursor, only a weak decrease in the seismicity rate would be observed.

4.2. Spatial Extent of the Quiescence Anomalies

[31] The spatial extent of quiescence anomalies has usually not been very well defined in previous studies on great subduction zone earthquakes. In particular, it has been unclear whether the quiescence areas are larger or smaller than the asperities ruptured by a subsequent main shock. From the present results, it is obvious that the spatial extents of the anomalies are smaller than the 2003 Tokachi-oki asperities and the quiescence anomalies are located in and around the northeastern boundary of the asperities (Figure 6).

4.3. Duration of the Quiescence Anomalies

[32] The duration of quiescence is well defined because the onset time is sharp. The duration is defined as the time between the onset of quiescence and the main shock. In this study, the duration of quiescence is found to be 4.2–4.9 years for the Tokachi-oki earthquake ($M_w = 8.3$) in 2003. This is similar to periods of quiescence before other great (Global CMT M_w~8) subduction earthquakes: 5.3 years for the Kermadec earthquake ($M_w = 7.9$) in 1976 [*Wyss et al.*, 1984], 3.8–5.5 years for the Andreanof Island earthquake ($M_w = 7.9$) in 1986 [*Kisslinger*, 1988] and 5.3–6.0 years for the Hokkaido-Toho-oki earthquake ($M_w = 8.3$) in 1994 [*Katsumata and Kasahara*, 1999]. In the case of the Andreanof Island earthquake, the duration of quiescence was 3.8 years based on the earthquake catalog of the Central Aleutian Seismic Network (CASN) [*Kisslinger*, 1988]. However, the duration was 5.5 years based on the Helicorder records of the station Adak, which allowed an earthquake count independent from the CASN catalog [*Wyss*, 1991]. Therefore, the quiescence duration for the Andreanof Island earthquake can be considered to be 3.8–5.5 years. These observations might imply that the characteristic precursor time is about 5 years for M~8 subduction zone earthquakes. On the other hand, these limits may be imposed artificially by the data. Because the earthquake catalog used in this study covers only 10 years, it may not be possible to define quiescence anomalies with durations of 10 years, even if they existed. Actually, *Takahashi and Kasahara* [2004] pointed out that the number of earthquakes with $M \geq 5.0$ decreased in the focal area of the 2003 Tokachi-oki earthquake, based on the 50-years-long JMA catalog. The quiescence started around 1990, and lasted about 14 years until the main shock. Using the data from *Takahashi and Kasahara* [2004, Figure 3], the Z-values can be calculated, and they are found to be very small: $Z = +2.8$ when $T_s = 1990.0$ and $T_w = 8$ years; $Z = +1.5$ when $T_s = 1990.0$ and $T_w = 10$ years; and $Z = +1.7$ when $T_s = 1991.0$ and $T_w = 12$ years. These small Z-values suggest that the quiescence pointed out by *Takahashi and Kasahara* [2004] was not statistically significant. As shown in section 5.5, even Z~4.0 is too small to deny the possibility that the seismic quiescence occurred by chance in association with the 2003 Tokachi-oki earthquake. *Katsumata and Kasahara* [1999] found that the duration of quiescence was 5.3 years before the Hokkaido-Toho-oki earthquake ($M_w = 8.3$) in 1994 based on the 50-years-long International Seismological Center catalog. Since the Z-value was +6.8 in that case, it was statistically significant. Moreover, a hypothesis that precursor time is a function of the main shock magnitude has been put forward by some authors [e.g., *Scholz et al.*, 1973; *Rikitake*, 1975; *Wyss and Habermann*, 1988]. More reliable case studies are required to strengthen the statistical basis of this hypothesis.

5. Concluding Remarks

[33] Around 50 years ago, *Mogi* [1969] presented a seismic quiescence hypothesis that the seismicity rate decreases several years prior to large and great earthquakes. Many authors have attempted to provide support for this hypothesis using various earthquake catalogs. It is, however, difficult to detect reliable, genuine changes in the seismicity rate because of man-made artifacts. In the present study, all hypocenters and magnitudes are re-determined to reduce such effects in the earthquake catalog. As a result, a decrease in seismic activity is detected, that exhibits a strong temporal and spatial association with the asperity ruptured by the 2003 Tokachi-oki earthquake. This can thus be considered to be good evidence for a precursory seismic quiescence anomaly. Although current studies on seismic quiescence detection before great earthquakes are very limited, it is likely that it is commonly associated with subduction zone great earthquakes. Improved monitoring of such quiescence is therefore of the utmost importance for future intermediate-term earthquake prediction.

[34] **Acknowledgments.** I thank Stefan Wiemer for providing the ZMAP software, and Shinzaburo Ozawa for the afterslip data. GMT-SYSTEM [*Wessel and Smith*, 1991] was used for data mapping. MICAP-G [*Naito and Yoshikawa*, 1999] was used to calculate changes in the Coulomb

failure stress. Comments from Bogdan Enescu, Rodolfo Console, Robert Nowack, Takuji Yamada, and anonymous reviewers have been very helpful in revising the manuscript. I thank four engineers at ISV for maintaining the seismographic network: Masayoshi Ichiyanagi, Muneo Okayama, Masamitsu Takada, and Teruhiro Yamaguchi.

References

Aoi, S., B. Enescu, W. Suzuki, Y. Asano, K. Obara, T. Kunugi, and K. Shiomi (2010), Stress transfer in the Tokai subduction zone from the 2009 Suruga Bay earthquake in Japan, *Nat. Geosci.*, *3*, 496–500, doi:10.1038/ngeo885.

Baba, T., and T. Hori (2006), Heterogeneous interplate coupling in the southern Kuril subduction zone inferred from back slip inversion analysis with the minimum solution norm constraint, *Eos Trans. AGU*, *87*(36), West. Pac. Geophys. Meet. Suppl., Abstract T12A–04.

Baba, T., K. Hirata, T. Hori, and H. Sakaguchi (2006), Offshore geodetic data conducive to the estimation of the afterslip distribution following the 2003 Tokachi-oki earthquake, *Earth Planet. Sci. Lett.*, *241*, 281–292, doi:10.1016/j.epsl.2005.10.019.

Dieterich, J. (1994), A constitutive law for rate of earthquake production and its application to earthquake clustering, *J. Geophys. Res.*, *99*, 2601–2618, doi:10.1029/93JB02581.

Enescu, B., and K. Ito (2001), Some premonitory phenomena of the 1995 Hyogo-ken Nanbu earthquake: Seismicity, *b*-value and fractal dimension, *Tectonophysics*, *338*, 297–314, doi:10.1016/S0040-1951(01)00085-3.

Fukuyama, E., S. Ishida, D. S. Dreger, and H. Kawai (1998), Automated seismic moment tensor determination by using on-line broadband seismic waveforms (in Japanese with English abstract), *J. Seismol. Soc. Jpn.*, *2*, 149–156.

Gutenberg, R., and C. F. Richter (1944), Frequency of earthquakes in California, *Bull. Seismol. Soc. Am.*, *34*, 185–188.

Habermann, R. E. (1987), Man-made changes of seismicity rates, *Bull. Seismol. Soc. Am.*, *77*, 141–157.

Habermann, R. E. (1991), Seismicity rate variations and systematic changes in magnitudes in teleseismic catalogs, *Tectonophysics*, *193*, 277–289, doi:10.1016/0040-1951(91)90337-R.

Habermann, R. E., and F. Creamer (1994), Catalog errors and the M8 earthquake prediction algorithm, *Bull. Seismol. Soc. Am.*, *84*, 1551–1559.

Hamada, N., and Y. Suzuki (2004), Re-examination of aftershocks of the 1952 Tokachi-oki earthquake and a comparison with those of the 2003 Tokachi-oki earthquake, *Earth Planets Space*, *56*, 341–345.

Hirata, K., Y. Tanioka, K. Satake, S. Yamaki, and E. L. Geist (2004), The tsunami source area of the 2003 Tokachi-oki earthquake estimated from tsunami travel times and its relationship to the 1952 Tokachi-oki earthquake, *Earth Planets Space*, *56*, 367–372.

Hirata, N., and M. Matsu'ura (1987), Maximum-likelihood estimation of hypocenter with origin time eliminated using nonlinear inversion technique, *Phys. Earth Planet. Inter.*, *47*, 50–61, doi:10.1016/0031-9201(87)90066-5.

Hirose, H. (2004), Hi-net tiltmeter records prior to the 2003 Tokachi-oki earthquake (in Japanese), *Rep. Coord. Comm. Earthquake Predict.*, *71*, 194–202.

Ide, S., and M. Takeo (1996), The dynamic rupture process of the 1993 Kushiro-oki earthquake, *J. Geophys. Res.*, *101*, 5661–5675, doi:10.1029/95JB00959.

Irwin, M., F. Kimata, K. Hirahara, T. Sagiya, and A. Yamagiwa (2004), Measuring ground deformations with 1-Hz GPS data: The 2003 Tokachi-oki earthquake (preliminary report), *Earth Planets Space*, *56*, 389–393.

Ishimoto, M., and K. Iida (1939), Observations of earthquakes registered with the microseimograph constructed recently, *Bull. Earthquake Res. Inst. Univ. Tokyo*, *17*, 443–478.

Kato, N. (2003), A possible model for large preseismic slip on a deeper extension of a seismic rupture plane, *Earth Planet. Sci. Lett.*, *216*, 17–25, doi:10.1016/S0012-821X(03)00483-7.

Kato, N., M. Ohtake, and T. Hirasawa (1997), Possible mechanism of precursory seismic quiescence: Regional stress relaxation due to preseismic sliding, *Pure Appl. Geophys.*, *150*, 249–267, doi:10.1007/s000240050075.

Katsumata, K., and M. Kasahara (1999), Precursory seismic quiescence before the 1994 Kurile earthquake (M_w = 8.3) revealed by three independent seismic catalogs, *Pure Appl. Geophys.*, *155*, 443–470, doi:10.1007/s000240050274.

Katsumata, K., and M. Kasahara (2004), Apparent change in b-value of the frequency-magnitude relation in the seismic catalog of Hokkaido Univ, (in Japanese), *J. Seismol. Soc. Jpn.*, *56*, 537–540.

Katsumata, K., M. Kasahara, S. Ozawa, and A. Ivashchenko (2002), A five years super-slow aseismic precursor model for the 1994 M8.3 Hokkaido-Toho-Oki lithospheric earthquake based on tide gauge data, *Geophys. Res. Lett.*, *29*(13), 1654, doi:10.1029/2002GL014982.

Katsumata, K., N. Wada, and M. Kasahara (2003), Newly imaged shape of the deep seismic zone within the subducting Pacific plate beneath the Hokkaido corner, Japan-Kurile arc-arc junction, *J. Geophys. Res.*, *108*(B12), 2565, doi:10.1029/2002JB002175.

Kisslinger, C. (1988), An experiment in earthquake prediction and the 7 May 1986 Andreanof Island earthquake, *Bull. Seismol. Soc. Am.*, *78*, 218–229.

Linde, A. T., and I. S. Sacks (2002), Slow earthquakes and great earthquakes along the Nankai trough, *Earth Planet. Sci. Lett.*, *203*, 265–275, doi:10.1016/S0012-821X(02)00849-X.

Miyazaki, S., P. Segall, J. Fukuda, and T. Kato (2004), Space time distribution of afterslip following the 2003 Tokachi-oki earthquake: Implications for variations in fault zone frictional properties, *Geophys. Res. Lett.*, *31*, L06623, doi:10.1029/2003GL019410.

Mogi, K. (1969), Some feature of recent seismic activity in and near Japan (2), Activity before and after great earthquakes, *Bull. Earthquake Res. Inst. Univ. Tokyo*, *47*, 395–417.

Mogi, K. (1985), Temporal variation of crustal deformation during the days preceding a thrust-type great earthquake: The 1944 Tonankai earthquake of magnitude 8 in Japan, *Pure Appl. Geophys.*, *122*, 765–780, doi:10.1007/BF00876383.

Moriya, T., T. Mogi, and M. Takada (2010), Anomalous pre-seismic transmission of VHF-band radio waves resulting from large earthquakes, and its statistical relationship to magnitude of impending earthquakes, *Geophys. J. Int.*, *180*, 858–870, doi:10.1111/j.1365-246X.2009.04461.x.

Naito, H., and S. Yoshikawa (1999), A program to assist crustal deformation analysis (in Japanese), *J. Seismol. Soc. Jpn.*, *52*, 101–103.

Nakaya, S. (2006), Spatiotemporal variation in *b* value within the subducting slab prior to the 2003 Tokachi-oki earthquake (*M* 8.0), Japan, *J. Geophys. Res.*, *111*, B03311, doi:10.1029/2005JB003658.

Ogata, Y. (2005), Synchronous seismicity changes in and around the northern Japan preceding the 2003 Tokachi-oki earthquake of *M*8.0, *J. Geophys. Res.*, *110*, B08305, doi:10.1029/2004JB003323.

Ohtake, M., T. Matsumoto, and G. V. Latham (1977), Seismicity gap near Oaxaca, Southern Mexico as a probable precursor to a large earthquake, *Pure Appl. Geophys.*, *115*, 375–385, doi:10.1007/BF01637115.

Okada, Y. (1992), Internal deformation due to shear and tensile faults in a half-space, *Bull. Seismol. Soc. Am.*, *82*, 1018–1040.

Ozawa, S., M. Kaidzu, M. Murakami, T. Imakiire, and Y. Hatanaka (2004), Coseismic and postseismic crustal deformation after the M_w 8 Tokachi-oki earthquake in Japan, *Earth Planets Space*, *56*, 675–680.

Parsons, T., C. Ji, and E. Kirby (2008), Stress changes from the 2008 Wenchuan earthquake and increased hazard in the Sichuan basin, *Nature*, *454*, 509–510, doi:10.1038/nature07177.

Rikitake, T. (1975), Earthquake precursors, *Bull. Seismol. Soc. Am.*, *65*, 1133–1162.

Sato, T., et al. (2004), Changes in groundwater level associated with the 2003 Tokachi-oki earthquake, *Earth Planets Space*, *56*, 395–400.

Scholz, C. H. (1988), Mechanisms of seismic quiescence, *Pure Appl. Geophys.*, *126*, 701–718, doi:10.1007/BF00879016.

Scholz, C. H., L. R. Sykes, and Y. P. Aggarval (1973), Earthquake prediction: A physical basis, *Science*, *181*, 803–810, doi:10.1126/science.181.4102.803.

Segall, P., E. K. Desmarais, D. Shelly, A. Miklius, and P. Cervelli (2006), Earthquakes triggered by silent slip events on Kīlauea volcano, Hawaii, *Nature*, *442*, 71–74, doi:10.1038/nature04938.

Shinohara, M., et al. (2004), Aftershock observation of the 2003 Tokachi-oki earthquake by using dense ocean bottom seismometer network, *Earth Planets Space*, *56*, 295–300.

Stein, R. S. (1999), The role of stress transfer in earthquake occurrence, *Nature*, *402*, 605–609, doi:10.1038/45144.

Stein, R. S., and M. Lisowski (1983), The 1979 Homestead Valley earthquake sequence, California: Control of aftershocks and postseismic deformation, *J. Geophys. Res.*, *88*, 6477–6490, doi:10.1029/JB088iB08p06477.

Stuart, W. D. (1979), Strain softening prior to two-dimensional strike slip earthquakes, *J. Geophys. Res.*, *84*, 1063–1070, doi:10.1029/JB084iB03p01063.

Suzuki, S., T. Takanami, Y. Motoya, and I. Nakanishi (1988), A real-time automatic processing system of seismic waves for the network of Hokkaido Univ (in Japanese), *J. Seismol. Soc. Jpn.*, *41*, 359–373.

Takahashi, H., and M. Kasahara (2004), The 2003 Tokachi-oki earthquake off southeastern Hokkaido, Japan–seismic activity from the former 1952 Tokachi-oki earthquake, foreshock, mainshock, aftershocks, and triggered earthquakes, (in Japanese), *J. Seismol. Soc. Jpn.*, *57*, 115–130.

Tanioka, Y., K. Hirata, R. Hino, and T. Kanazawa (2004), Slip distribution of the 2003 Tokachi-oki earthquake estimated from tsunami waveform inversion, *Earth Planets Space*, *56*, 373–376.

Uchida, N., S. Yui, S. Miura, T. Matsuzawa, A. Hasegawa, Y. Motoya, and M. Kasahara (2009), Quasi-static slip on the plate boundary associated with the 2003 M8.0 Tokachi-oki and 2004 M7.1 off-Kushiro earthquakes, Japan, *Gondwana Res.*, *16*, 527–533, doi:10.1016/j.gr.2009.04.002.

Urabe, T., and S. Tsukada (1992), WIN- a workstation program for processing waveform data from microearthquake networks (abstract in Japanese), *Seismol. Soc. Jpn.*, *2*, 331.

Utsu, T. (1999), Representation and analysis of the earthquake size distribution: A historical review and some new approaches, *Pure Appl. Geophys.*, *155*, 509–535, doi:10.1007/s000240050276.

Watanabe, H. (1971), Determination of earthquake magnitude at regional distance in and near Japan (in Japanese), *J. Seismol. Soc. Jpn.*, *32*, 281–296.

Wessel, P., and W. H. F. Smith (1991), Free software helps map and display data, *Eos Trans. AGU*, *72*(41), 441, doi:10.1029/90EO00319.

Wiemer, S. (1996), Analysis of seismicity: New technique and case studies, Ph.D. dissertation, 151 pp., Univ. of Alaska Fairbanks, Fairbanks, Alaska.

Wiemer, S. (2001), A software package to analyze seismicity: ZMAP, *Seismol. Res. Lett.*, *72*(3), 373–382, doi:10.1785/gssrl.72.3.373.

Wiemer, S., and M. Wyss (1994), Seismic quiescence before the Landers (M = 7.5) and Big Bare (M = 6.5) 1992 earthquakes, *Bull. Seismol. Soc. Am.*, *84*, 900–916.

Wiemer, S., and M. Wyss (2000), Minimum magnitude of completeness in earthquake catalogs: Examples from Alaska, the western United States, and Japan, *Bull. Seismol. Soc. Am.*, *90*, 859–869, doi:10.1785/0119990114.

Wyss, M. (1985), Precursors to large earthquakes, *Earthquake Predict. Res.*, *3*, 519–543.

Wyss, M. (1986), Seismic quiescence precursor to the 1983 Kaoiki (Ms = 6.6), Hawaii, earthquake, *Bull. Seismol. Soc. Am.*, *76*, 785–800.

Wyss, M. (1991), Reporting history of the central Aleutians seismograph network and the quiescence preceding the 1986 Andreanof Island earthquake, *Bull. Seismol. Soc. Am.*, *81*, 1231–1254.

Wyss, M., and R. O. Burford (1985), Current episodes of seismic quiescence along the San Andreas fault between San Juan Bautista and Stone Canyon, California: Possible precursors to local moderate mainshocks?, *U.S. Geol. Surv. Open File Rep.*, *85–745*, 376–426.

Wyss, M., and R. O. Burford (1987), Occurrence of a predicted earthquake on the San Andreas fault, *Nature*, *329*, 323–325, doi:10.1038/329323a0.

Wyss, M., and R. E. Habermann (1988), Precursory seismic quiescence, *Pure Appl. Geophys.*, *126*, 319–332, doi:10.1007/BF00879001.

Wyss, M., and A. H. Martirosyan (1998), Seismic quiescence before the M7, 1988, Spitak earthquake, Armenia, *Geophys. J. Int.*, *134*, 329–340, doi:10.1046/j.1365-246x.1998.00543.x.

Wyss, M., R. E. Habermann, and J. C. Griesser (1984), Seismic quiescence and asperities in the Tonga-Kermadec arc, *J. Geophys. Res.*, *89*, 9293–9304, doi:10.1029/JB089iB11p09293.

Wyss, M., K. Shimazaki, and T. Urabe (1996), Quantitative mapping of a precursory quiescence to the Izu-Oshima 1990(M = 6.5) earthquake, Japan, *Geophys. J. Int.*, *127*, 735–743, doi:10.1111/j.1365-246X.1996.tb04052.x.

Yagi, Y. (2004), Source rupture process of the 2003 Tokachi-oki earthquake determined by joint inversion of teleseismic body wave and strong ground motion data, *Earth Planets Space*, *56*, 311–316.

Yamanaka, Y., and M. Kikuchi (2003), Source process of the recurrent Tokachi-oki earthquake on September 26, 2003, inferred from teleseismic body waves, *Earth Planets Space*, *55*, e21–e24.

Yoshida, S., and N. Kato (2003), Episodic aseismic slip in a two-degree-of-freedom blockspring model, *Geophys. Res. Lett.*, *30*(13), 1681, doi:10.1029/2003GL017439.

Zhuang, J., Y. Ogata, and D. Vere-Jones (2002), Stochastic declustering of space-time earthquake occurrences, *J. Am. Stat. Assoc.*, *97*(458), 369–380, doi:10.1198/016214502760046925.

Zuniga, F. R., and S. Wiemer (1999), Seismicity patterns: Are they always related to natural causes?, *Pure Appl. Geophys.*, *155*, 713–726, doi:10.1007/s000240050285.

K. Katsumata, Institute of Seismology and Volcanology, Hokkaido University, North-10 West-8, Sapporo 060-0810, Japan. (kkatsu@mail.sci.hokudai.ac.jp)